Available online at www.sciencedirect.com
ScienceDirect
ELSEVIER
Engineering Geology 89 (2007) 67 – 87
ENGINEERING GEOLOGY
www.elsevier.com/locate/enggeo

Landslide susceptibility revealed by LIDAR imagery and historical records, Seattle, Washington ☆

William H. Schulz *

U.S. Geological Survey, Box 25046, MS-966, Denver, CO 80225-0046, United States

Received 28 April 2006; received in revised form 31 August 2006; accepted 19 September 2006
Available online 15 November 2006

Abstract

Light detection and ranging (LIDAR) data were used to visually map landslides, headscarps, and denuded slopes in Seattle, Washington. Four times more landslides were mapped than by previous efforts that used aerial photographs. The mapped landforms (landslides, headscarps, and denuded slopes) were created by many individual landslides. The spatial distribution of mapped landforms and 1308 historical landslides show that historical landslide activity has been concentrated on the mapped landforms, and that most of the landslide activity that created the landforms was prehistoric. Thus, the spatial densities of historical landslides on the landforms provide approximations of the landforms' relative susceptibilities to future landsliding. Historical landslide characteristics appear to be closely related to landform type so relative susceptibilities were determined for landslides with various characteristics. No strong relations were identified between stratigraphy and landslide occurrence; however, landslide characteristics and slope morphology appear to be related to stratigraphic conditions.

Human activity is responsible for causing about 80% of historical Seattle landslides. The distribution of mapped landforms and human-caused landslides suggests the probable characteristics of future human-caused landslides on each of the landforms. The distribution of mapped landforms and historical landslides suggests that erosion of slope-toes by surface water has been a necessary condition for causing Seattle landslides. Human activity has largely arrested this erosion, which implies that landslide activity will decrease with time as hillsides naturally stabilize. However, evaluation of glacial-age analogs of areas of recent slope-toe erosion suggests that landslide activity in Seattle will continue for the foreseeable future.

Keywords: Landslide; LIDAR; Geomorphology; Seattle; Washington; Coastal bluff; Historical records

1. Introduction

Landslides commonly cause property damage and occasionally human casualties in the Seattle, Washington area (Fig. 1). The hazard posed by landslides in Seattle has been so significant that city agencies began maintaining landslide records in 1890 (Laprade et al., 2000) when the city's population was only about 5000 people (www.historylink.org). These records have been cataloged in a historical landslide dat abase containing 1433 entries of landslides reported between 1890 and 2003 (Laprade et al., 2000; Shannon and Wilson, Inc., 2003). Although measures have been taken in Seattle to promote land use, development, and construction practices that do not exacerbate the landslide problem, the relative proportion of human-

☆ The use of trade, product, industry, or firm names is for descriptive purposes only and does not imply endorsement by the US Government.

* Tel.: +1 303 273 8404; fax: +1 303 273 8600.
E-mail address: wschulz@usgs.gov.

0013-7952/$ - see front matter © 2006 Elsevier B.V. All rights reserved.
doi:10.1016/j.enggeo.2006.09.019

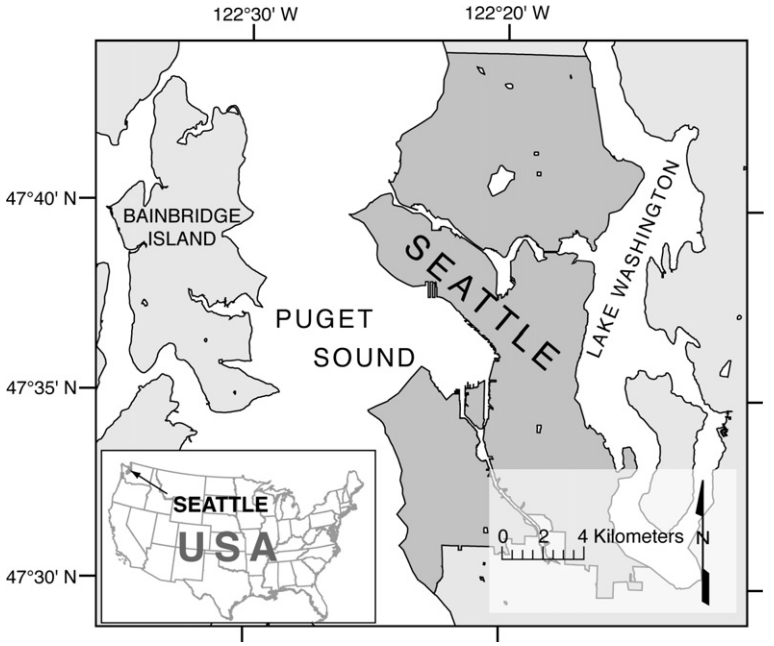

Fig. 1. Map showing the location of Seattle in relation to Puget Sound, Lake Washington, and Bainbridge Island.

caused landslides has increased significantly since the 1980s (Schulz, 2005).

The continuing occurrence of destructive landslides in Seattle may be partly due to a lack of recognition of landslide-prone terrain and incomplete understanding of the necessary conditions that result in Seattle landslides. Geologic, coastal, and landslide-specific maps of Seattle (Waldron et al., 1962; Waldron, 1967; Youngmann, 1979; Yount et al., 1993; Wait, 2001) identify only a very small part of the total area in which historical landslides have been reported (Schulz, 2004, 2005). These maps were constructed using aerial photographs, ground-based study, and historical records. Several studies have postulated that coastal erosion contributes to landsliding in the Seattle area (e.g., Thorsen, 1989; Hampton et al., 2004), although most of these conclude that since the majority of the Seattle shoreline has been protected from wave attack by human activities, coastal erosion is no longer a factor in landslide occurrence (e.g., Galster and Laprade, 1991; Shipman, 2004). Following significant landslide events of the early 1970s, Tubbs (1974, 1975) concluded that landslide activity in Seattle is typically caused by high pore-water pressures that occur near the basal contact of the Vashon advance outwash (also referred to as Esperance Sand, Mullineaux et al., 1965). Tubbs (1974, 1975) mapped a 61-m-wide strip centered along this contact as a zone of particular landslide hazard. Tubbs' conclusion has been advanced by many scientists and engineers (e.g., Galster and Laprade, 1991; Gerstel et al., 1997; Laprade et al., 2000; Savage et al., 2000; Coe et al., 2000; Wait, 2001; Montgomery et al., 2001; Coe et al., 2004; Shipman, 2004) and adopted by the City of Seattle for regulating development of landslide-prone terrain. However, only 29% of historical landslides (Shannon and Wilson, Inc., 2003) occur within the contact strip (using the contact as mapped by Troost et al., 2005), an equal percentage occurred on Seattle-zoned steep slopes (>40% inclination and 3.3 m height) located outside of the contact strip, and 30% occurred within zoned areas of concentrated historical landsliding (Laprade et al., 2000). The performance of Seattle zoning in assisting identification of the causes of landslides demonstrates that landslide occurrence in Seattle is not fully understood.

The dense vegetation typical of the Seattle area (Fig. 2) obscures the morphology of landslides both in the field and in aerial photography. Light detection and ranging (LIDAR) data can be processed to reveal the topography beneath vegetation and has proven useful in the Puget Sound region for identifying tectonic fault scarps (Haugerud et al., 2003; Johnson et al., 2003; Sherrod et al., 2004), previously unmapped landslides, and other geomorphic landforms (Haugerud et al., 2003). The present study sought to: 1) create a landslide inventory map for Seattle using LIDAR-derived imagery and to evaluate the relative quality of the LIDAR-derived map against previous Seattle landslide inventory maps created using aerial photographs, 2) create a landslide susceptibility map using LIDAR imagery and records of historical landslides,

Fig. 2. Photograph showing typical vegetation in Seattle covering a landslide complex. View is toward the southeast from south of West Point (Fig. 3) on June 14, 2005. The vertical escarpment is approximately 12 m high. Photo by Jeffery Coe (US Geological Survey).

and 3) evaluate results in the context of landslide causation in Seattle. A secondary goal of the present study was to perform an evaluation of the locations and characteristics of historical Seattle landslides and their relations to stratigraphic conditions and landslide-related landforms mapped using LIDAR imagery.

2. Setting of landslides in Seattle

Seattle occupies an isthmus between Puget Sound and Lake Washington and has an area of 215.6 km^2 (Fig. 3). The recent geologic history of the area includes cycles of Pleistocene glaciation followed by Holocene coastal erosion, stream incision, and grading by humans. Dominant landforms in Seattle are mostly glacial in origin and include elongate, north–south trending ridges and valleys sculpted by glacial ice, and former glacial outwash valleys and lake beds. These glacial landforms create a rolling upland surface, generally 50 or more meters above current sea level, that reflects the landscape present upon retreat of glacial ice and recession of meltwater (Figs. 3 and 4). The upland surface is locally truncated by bluffs along coastlines and drainages.

2.1. Post-glacial landscape evolution

Glaciers retreated from the Seattle area about 16,400 years ago (Booth, 1987; Booth et al., 2005). Glacial meltwaters were locally impounded, resulting in formation of lakes. Melt-off of the glaciers and other factors caused the relative levels of Puget Sound and Lake Washington to rise; about 6 to 10 m of rise occurred during the past 5000 years (Booth, 1987, Fig. 8; Sherrod et al., 2000). As is generally the case when surface-water bodies meet elevated land (e.g., Hampton et al., 2004), the rising levels of Puget Sound and Lake Washington resulted in erosion of the uplands by wave action and formation of coastal bluffs (Booth, 1987; Shipman, 2004) that truncate the glacially sculpted upland surface along most of the Seattle shoreline. Sea level rise since glacial melt-off has resulted in an estimated 150 to 900 m of retreat of Seattle's coastal bluffs, primarily by landsliding (Galster and Laprade, 1991; Shipman, 2004). Most of Seattle's coastal bluffs are no longer subjected to wave attack due to fill (human-constructed soil) placement along coasts, human lowering of the level of Lake Washington, and construction of shoreline protection structures.

The upland surface is incised throughout Seattle by drainages, many of which were produced during glacial melt-off (Booth et al., 2000; Troost et al., 2005) but now carry little or no water. Many drainages present during the late 1800s (Fig. 5) have since been filled or controlled by humans, thus the erosive power of Seattle streams has been greatly reduced.

Human activity has made Seattle perhaps the most graded city in North America (Galster and Laprade, 1991). Major grading activities in the latter part of the 19th and early part of the 20th centuries included

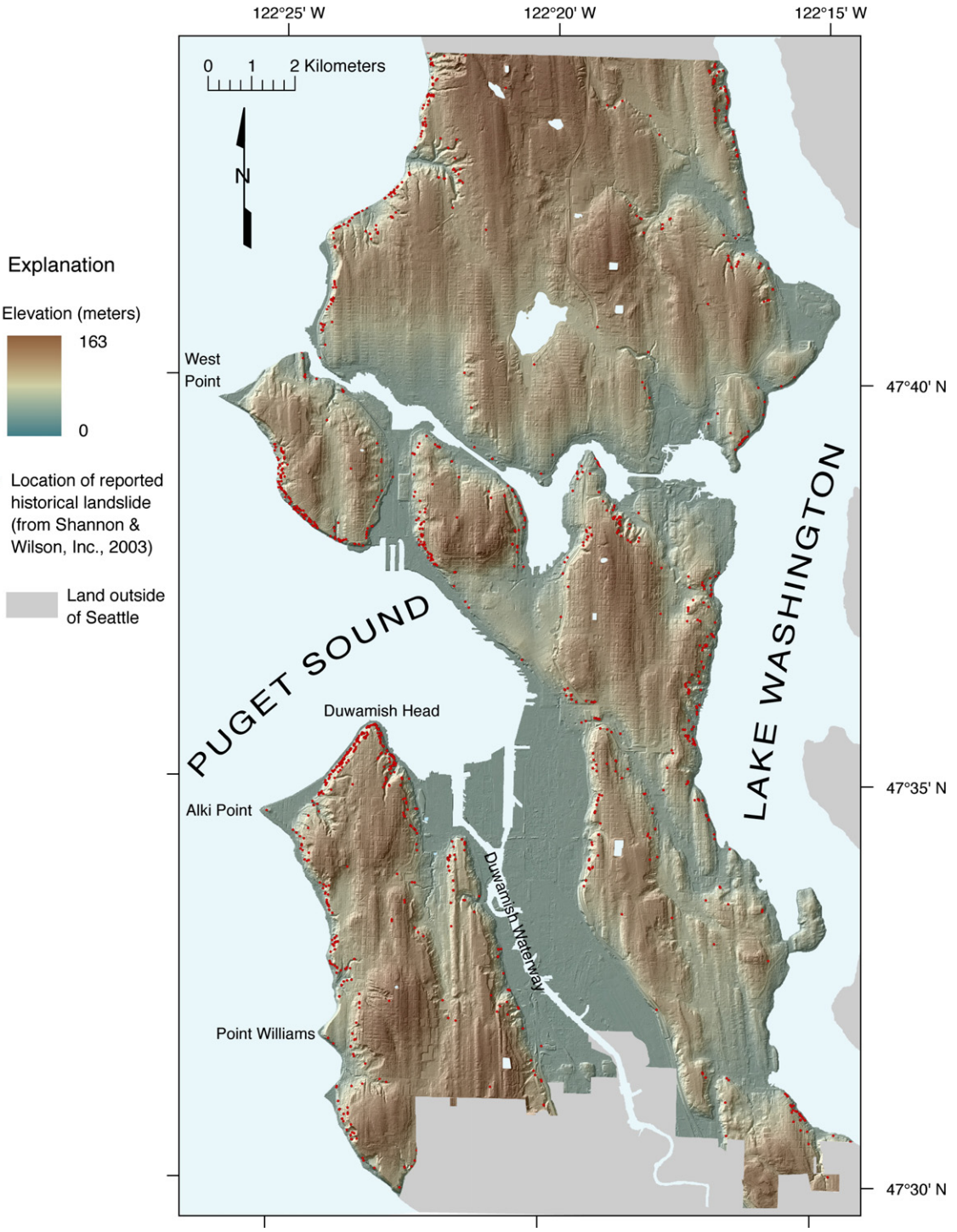

Fig. 3. Shaded relief map created from the LIDAR-derived, bare-earth digital elevation model (DEM) of Seattle showing land-surface elevations and locations of historical landslides (locations modified from Shannon and Wilson, Inc., 2003).

filling tidal flats, wetlands, and coastal areas to create more land area, and excavation of hills and filling of lowlands to flatten parts of the city. Grading has been so extensive that about 13 km of former coastal bluffs now appear as inland hills due to fill placement into Puget Sound (Fig. 5).

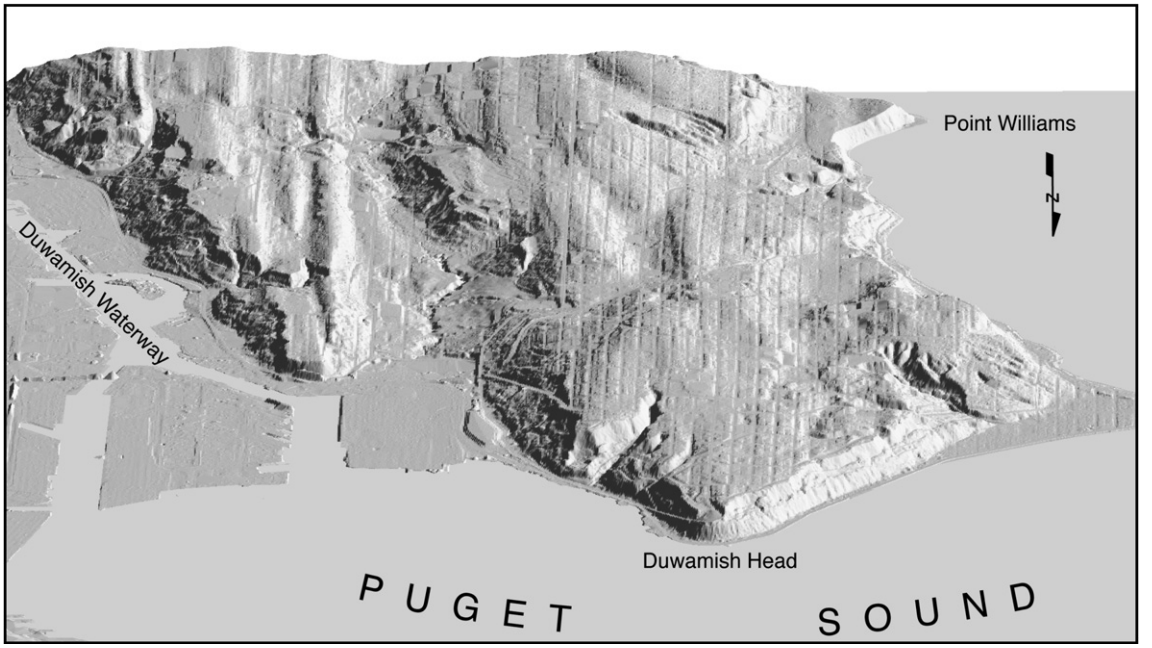

Fig. 4. Oblique aerial view created from the LIDAR-derived, bare-earth DEM with two times vertical exaggeration. View is toward the south of part of southwestern Seattle. The land area is approximately 4.6 km across at the top of the figure. The glaciated nature of the upland surface is highlighted by the north–south-oriented drumlins in the left part of the figure. The upland surface is truncated by bluffs along the Duwamish Waterway and Puget Sound, and by incised drainages, such as those near Duwamish Head and east (left) of Point Williams.

2.2. Topographic and geologic conditions

Seattle's coastal bluffs and slopes along drainages are up to 125 m high and are generally steepest at their crests along escarpments that usually range from 60° to vertical (Figs. 2–4). Slopes below the escarpments usually exceed about 30°. A sub-horizontal bench occurs about midslope along perhaps one-half of the bluffs and drainage slopes, below which the slopes are generally very steep (greater than 45°).

Stratigraphic units that underlie Seattle (Fig. 5) are primarily Pleistocene glacial outwash and till, and interglacial lacustrine and marine deposits, with Tertiary bedrock exposed in parts of southeastern Seattle (Troost et al., 2005). Beach and tidal deposits, alluvium, colluvium, landslide deposits, and fill (human-placed soil) locally overlie older stratigraphic units. Seattle's Pleistocene sediments are generally flat lying and laterally continuous, such that the stratigraphy beneath most of the city is similar. The youngest Pleistocene sediments result from the Vashon stade of the Fraser Glaciation (Armstrong et al., 1965), which occurred between about 16,400 and 17,400 years ago (Booth et al., 2005). According to Troost et al. (2005), Vashon recessional outwash deposits (Qvr) formed during glacial retreat, generally occupy low-lying parts of the upland surface (Fig. 5), and consist of stratified sand and gravel deposited by streams, and laminated silt and clay deposited in lakes. Vashon till (Qvt) caps most of the uplands and is typically a very dense, poorly sorted mixture of sand, silt, and gravel. Till is generally underlain by the Vashon advance outwash (Qva), which is comprised of well-sorted silty sand and gravel that was deposited in front of the advancing Vashon glacier. The basal contact of the advance outwash illustrates the flat-lying, laterally continuous characteristics of Seattle's Pleistocene deposits; this contact occurs on most hillsides that extend from near sea level to the uplands, and it can be continuously traced as far as 13 km (Fig. 5). The advance outwash is generally underlain by and grades into very dense, laminated clayey silt lacustrine deposits that comprise the Lawton Clay (Qvlc). Pre-Fraser age sedimentary deposits (Qpf) underlie the Lawton Clay and are comprised of a highly variable sequence of poorly to well-sorted gravel, sand, silt, and clay.

Two major aquifers underlie Seattle, one of which primarily occurs in the advance outwash (Qva) (Newcomb, 1952; Vaccaro et al., 1998). This aquifer is perched on the Lawton Clay (Qvlc) or on pre-Fraser deposits (Qpf) where the Lawton Clay is absent.

Because of its perched nature, groundwater flow within the advance outwash has a lateral component toward the margins of the isthmus and results in groundwater discharge onto slope faces and into overlying colluvium (Newcomb, 1952; Galster and Laprade, 1991; Vaccaro

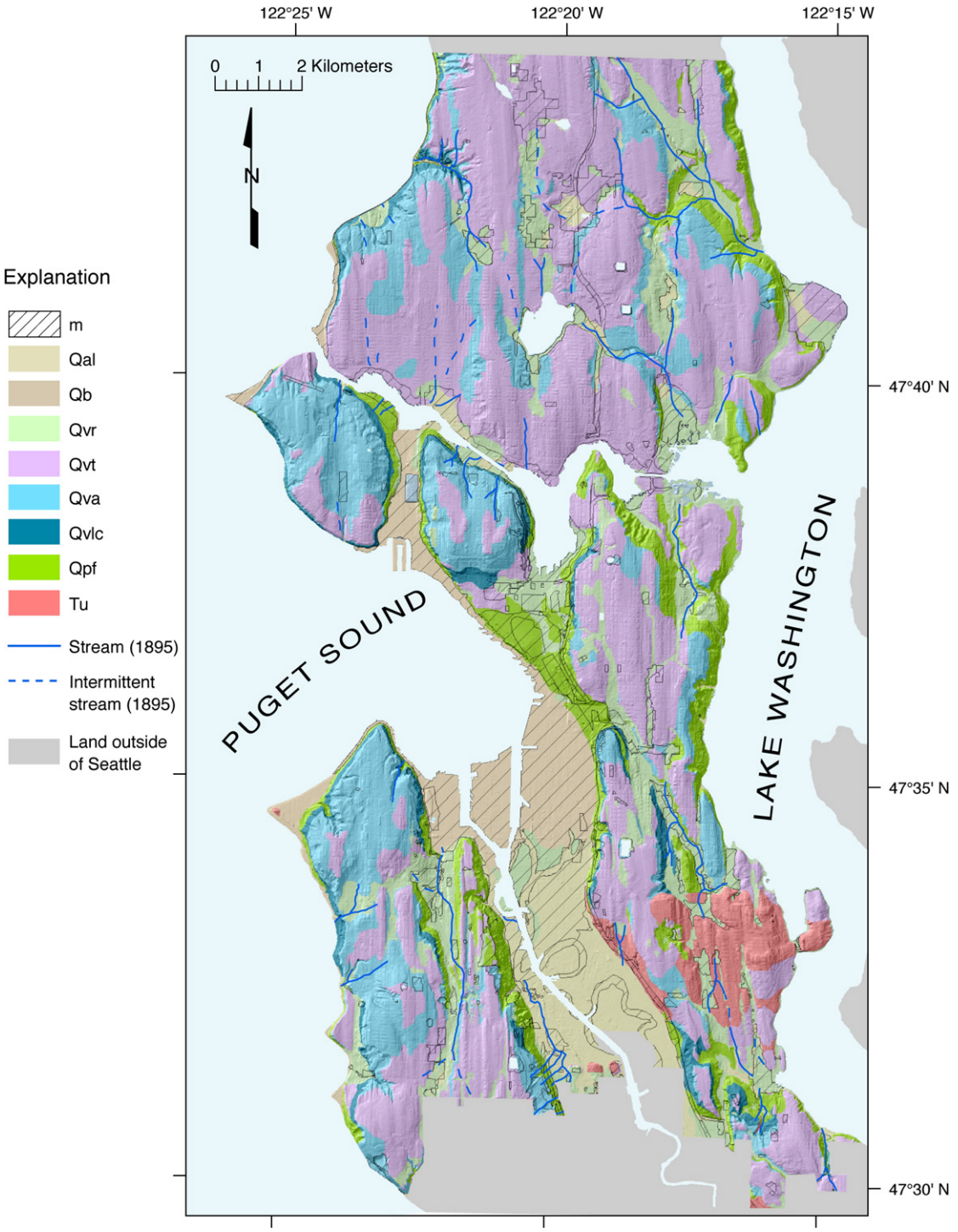

Fig. 5. Simplified geologic map of Seattle (simplified version of 1:12,000-scale maps, Troost et al., 2005) also modified to include late 19th century stream locations. Map units include: m = modified land (Holocene); Qal = alluvium and wetland deposits (Quaternary); Qb = beach and tide flat deposits (Quaternary). Deposits of the Vashon stade of the Fraser Glaciation (Pleistocene) include: Qvr = recessional outwash, lacustrine, ice-contact, and peat deposits; Qvt = till; Qva = advance outwash deposits; Qvlc = lacustrine deposits. Units older than the Vashon deposits include: Qpf = sedimentary deposits of pre-Fraser-glaciation age (Pleistocene); and Tu = sedimentary and volcanic bedrock units of Tertiary age. Streams were digitized from the U.S. Geological Survey Snohomish topographic quadrangle, 1:125,000 scale, 1895. Geology and streams are draped on a shaded relief map generated from the LIDAR-derived, bare-earth DEM.

et al., 1998). Based on the author's observations from boreholes and groundwater modeling, this discharge zone is generally from 3–26 m thick and its top is from 30–70 m below the upland surface. Groundwater also flows from the advance outwash downward through the Lawton Clay (Qvlc), where present, and recharges the aquifer that occurs in pre-Fraser deposits (Qpf) (Newcomb, 1952; Vaccaro et al., 1998).

Direct recharge from the advance outwash (Qva) to the pre-Fraser deposits (Qpf) occurs beneath perhaps one-third of Seattle where Lawton Clay (Qvlc) appears to be absent (Fig. 5).

3. Data and methods

3.1. Seattle LIDAR elevation data

LIDAR data for Seattle were acquired under the direction o f the Puget Sound LIDAR Consortium (PSLC). The LIDAR data were acquired November 1, 2000–April 1, 2001, which corresponds to the leaf-off period in Seattle. The data and description of their acquisition and processing are available at the PSLC website (http://pugetsoundlidar.org).

LIDAR ground-surface measurements for Seattle were acquired from aircraft at an average spacing of about 2 m (Haugerud and Harding, 2001). The data were processed to remove vegetation, buildings, and other aboveground features, thus creating a bare-earth digital elevation model (DEM) (the DEM used for the present study). The Seattle bare-earth DEM has vertical accuracy that is typically about 30 cm, but it is considerably less accurate in some areas, particularly those with dense vegetation because of reduced ground-surface measurements in these areas (Haugerud and Harding, 2001; PSLC, http://rocky2.ess.washington.edu/data/raster/lidar/lidar-data/index.html). The vertical error in these areas is as great as nearly 5 m, or about half the maximum vertical error identified in the USGS 10-m DEM (W.C. Haneberg, Haneberg Geoscience, pers. commun., 2005). Additionally, the corners between low-inclination and high-inclination surfaces were rounded during data processing, resulting in steep slopes whose crest and toe locations and overall inclination are not properly represented in the bare-earth DEM (Haugerud and Harding, 2001). The LIDAR bare-earth DEM data are in the Washington State Plane coordinate system and have a grid cell size of 1.8 m (6 ft).

3.2. Historical landslide data

Landslides in Seattle are concentrated along the coastal bluffs, but have also been reported on hillsides along drainages and on steep, glacially sculpted landforms (Waldron et al., 1962; Waldron, 1967; Tubbs, 1974; Youngmann, 1979; Yount et al., 1993; Harp et al., 1996; Gerstel et al., 1997; Baum et al., 1998; Laprade et al., 2000; Wait, 2001). Nearly all Seattle landslides are triggered by heavy winter precipitation (e.g., Tubbs, 1974, 1975; Galster and Laprade, 1991; Miller, 1991; Gerstel et al., 1997; Baum et al., 1998; Chleborad, 2000; Laprade et al., 2000; Montgomery et al., 2001; Coe et al., 2004). Historical records (Shannon and Wilson, Inc., 2003) show that 93% of reported landslides occurred between November 1 and April 30 (generally considered Seattle's winter rainy season). Earthquake-related ground shaking caused both small and very large landslides around A.D. 900 (Ludwin et al., 2005) and during 1949, 1965, and 2001 (Highland, 2003). Historical records also indicate that 80% of reported landslides have been at least partly caused by human activity.

Seattle landslides generally may be characterized as shallow slides, flows, and falls and topples (grouped and referred to as falls during this study), as well as deeper slides of earth and debris (terminology from Cruden and Varnes, 1996). The database of historical Seattle landslides (Shannon and Wilson, Inc., 2003) indicates that 72% were shallow (less than about 3 m thick). Shallow landslides in Seattle often have long, rapid runout and pose significant hazards to structures and humans located in their paths (Fig. 6). Deep landslides (greater than about 3 m thick) are the second most abundant type in Seattle (19%) and are usually slow moving and larger than shallow landslides so can adversely affect more structures. Flows are relatively uncommon in Seattle (6%), as are falls (3%). Eighty-five percent of historical Seattle landslides were small (less than 930 m^2 in area); 15% were large (greater than 930 m^2 in area). About 15% of historical landslides traveled rapidly at least 15 m from their initiation points; these landslides are referred to herein as long-runout landslides.

The historical landslide database was produced from records of various government agencies and those of Shannon and Wilson, Inc. (Laprade et al., 2000; Shannon and Wilson, Inc., 2003); only records for 1308 of the landslides were used during the present study (Fig. 3) because these landslides were located with certainty during creation of the database. Each landslide in the database is spatially represented by a point located at the approximate center of the headscarp (Laprade et al., 2000). The points are considered accurate to within 15 m (W.D. Nashem, Shannon and Wilson, Inc., pers. commun., 2004). The database provides attributes for each landslide (if they could be determined), such as date of

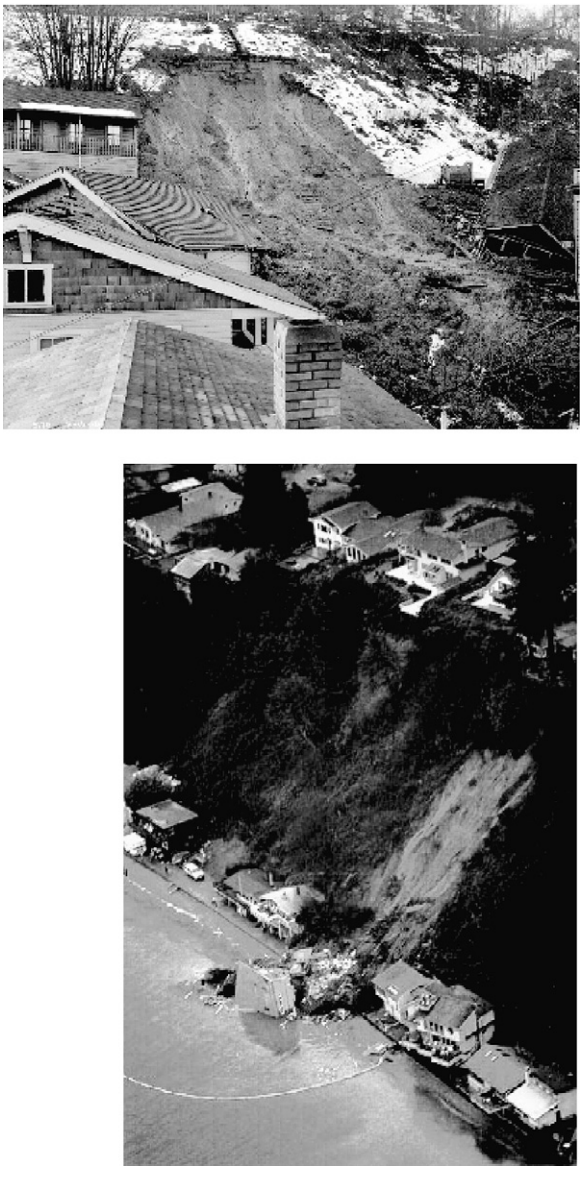

Fig. 6. Photographs of typical Seattle-area landslides. Top photograph is of a landslide that occurred in the area between Alki Point and Duwamish Head (Fig. 3) in 1916 (courtesy of Seattle municipal archives photograph collection, http://clerk.ci.seattle.wa.us/~public/phot1.htm). Bottom photograph is of a landslide that occurred on nearby Bainbridge Island (Fig. 1) in 1997 and killed a family of four (photograph by T. Tamura, The Seattle Times, used by permission).

occurrence, landslide type, size, and potential causes. During the present study, historical landslides were considered to have been human caused if records indicated that human activity had concentrated surface water or groundwater on or in the landslides, or if the landslides involved slopes excavated or loaded with soil by human activity.

Some damage was generally caused by each landslide in the database; landslides were typically not reported if they did not affect a built structure (Laprade et al., 2000; Coe et al., 2004). Therefore, the spatial distribution of landslides in the database is dependent on the history and density of land development in Seattle. Areas of Seattle where landslides have been reported were developed as early as the 1840s to as late as the 1960s. Hence, a bias toward greater spatial density of historical landslides likely exists in the database for areas that have been occupied longer. In addition, landslides on coastal bluffs and steep slopes along drainages may be reported less frequently than those that occur in the uplands because development of coastal bluffs and slopes along drainages is generally of lower density than that of the uplands.

The reporting bias present in the historical landslide database has greater adverse effects as the spatial distributions of historical landslides in smaller parts of Seattle are compared because of temporal settlement patterns that could suggest, for example, greater landslide density in a given area only because the area was inhabited longer. For the present study, the spatial distributions of historical landslides on landforms that are present throughout Seattle (not locally within Seattle) are compared so adverse effects of temporal settlement patterns should below. The landslide database bias due to development density probably has greater effect on the results of the present study. The effect should be a false indication of greater relative landslide susceptibility in areas that are presumably less susceptible (i.e., the more densely developed, relatively flat uplands).

A second limitation of the historical landslide database that could affect results of the present study is the representation of historical landslides as discrete points located at the centers of their headscarps. These points do not represent the entire areas covered by the respective landslides so the conditions present at each landslide (e.g., topography, geology) cannot be directly determined. This limitation should have little effect on the results of the present study because 85% of Seattle landslides are less than about 30 m across (based on small landslides being defined as less than 930 m^2 in area) and geologic conditions are assumed to generally be consistent within this small an area.

3.3. Mapping landslides and landforms using LIDAR imagery

Landslides (i.e., landslide deposits), headscarps, and denuded slopes were mapped from LIDAR-derived

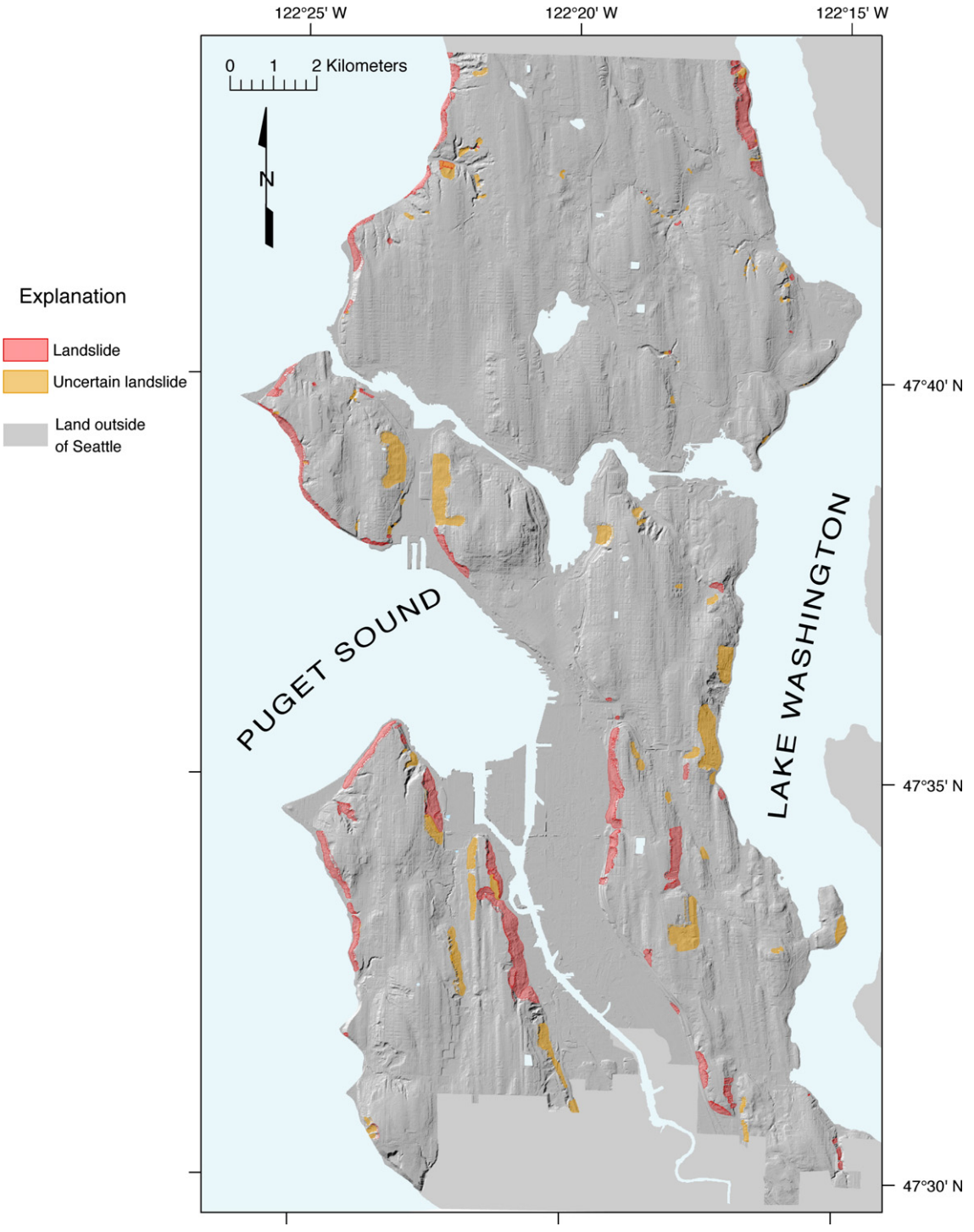

Fig. 7. Landslides mapped using LIDAR imagery (Schulz, 2004) draped on a shaded relief map generated from the LIDAR-derived, bare-earth DEM.

imagery because they are the primary landforms in Seattle created mainly by landslide activity. These landforms in all cases truncate the glacially sculpted upland surface (e.g., Fig. 4). Landslides and headscarps were only mapped when both could be identified for a given landslide; isolated headscarps or landslide deposits

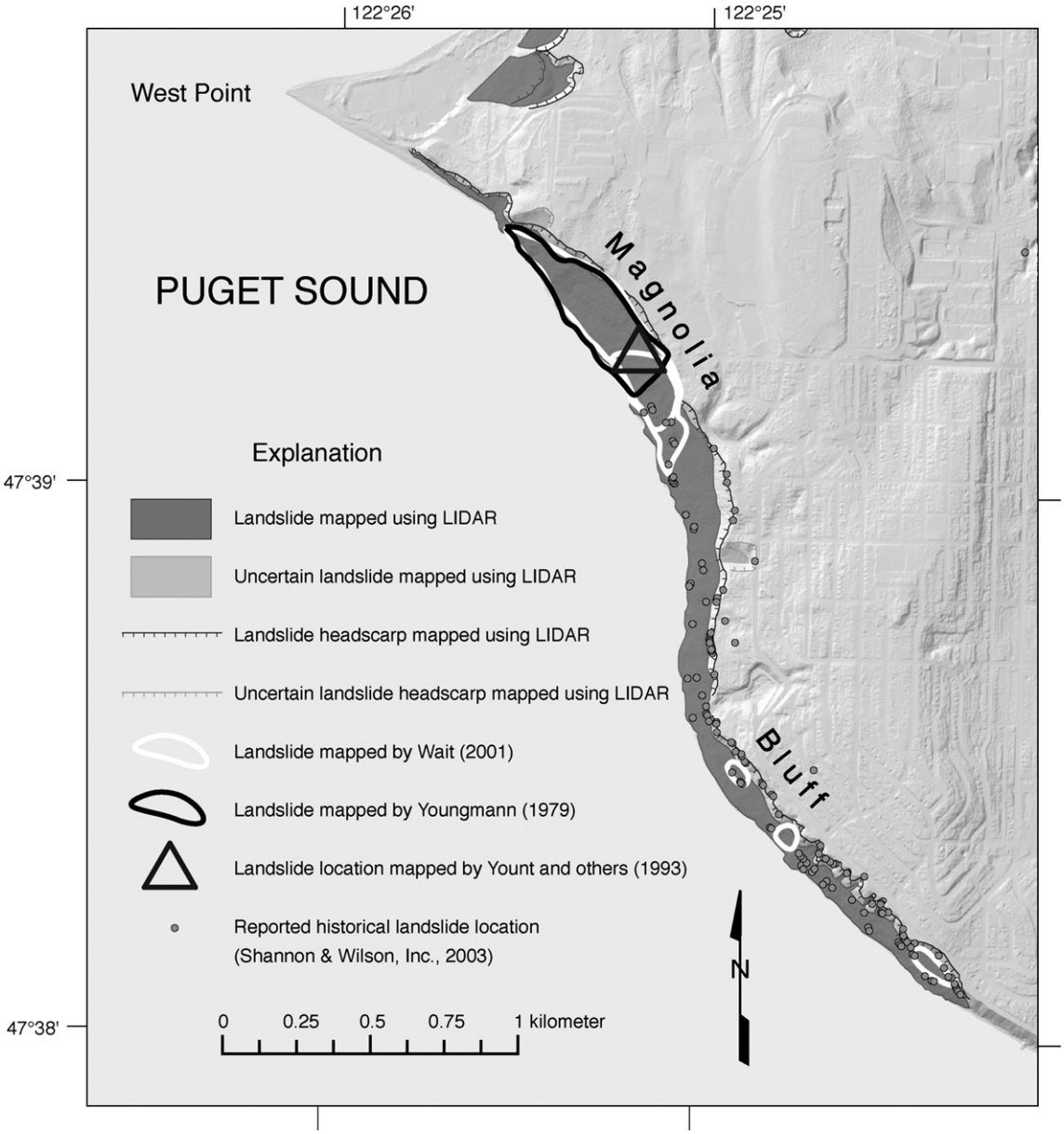

Fig. 8. Landslides along part of Magnolia Bluff near West Point (Fig. 3) that were mapped by Wait (2001), Youngmann (1979), Yount and others (1993), Shannon and Wilson, Inc. (2003), and by Schulz (2004) using LIDAR-derived imagery.

were not mapped. Denuded slopes are herein defined as slopes that formed by erosion and mass wasting (Bates and Jackson, 1987) following deglaciation, but which lack discernible deposits of individual landslides in the LIDAR imagery and usually also during ground-based study. Denuded slopes, therefore, were mapped where the glacial upland surface is truncated, but where landslides could not be identified. Field observations indicate that denuded slope areas probably lack discernible landslides because many Seattle landslides are too small and thin to be resolved by LIDAR and their deposits have often been removed or modified by erosion, mass wasting, and human activity.

Landform mapping was performed using an ESRI ArcInfo v. 8.3 –9.0 geographic information system (GIS). LIDAR-derived imagery that was used for mapping included shaded relief, slope, and topographic contour maps, as well as almost four-hundred topographic profiles.

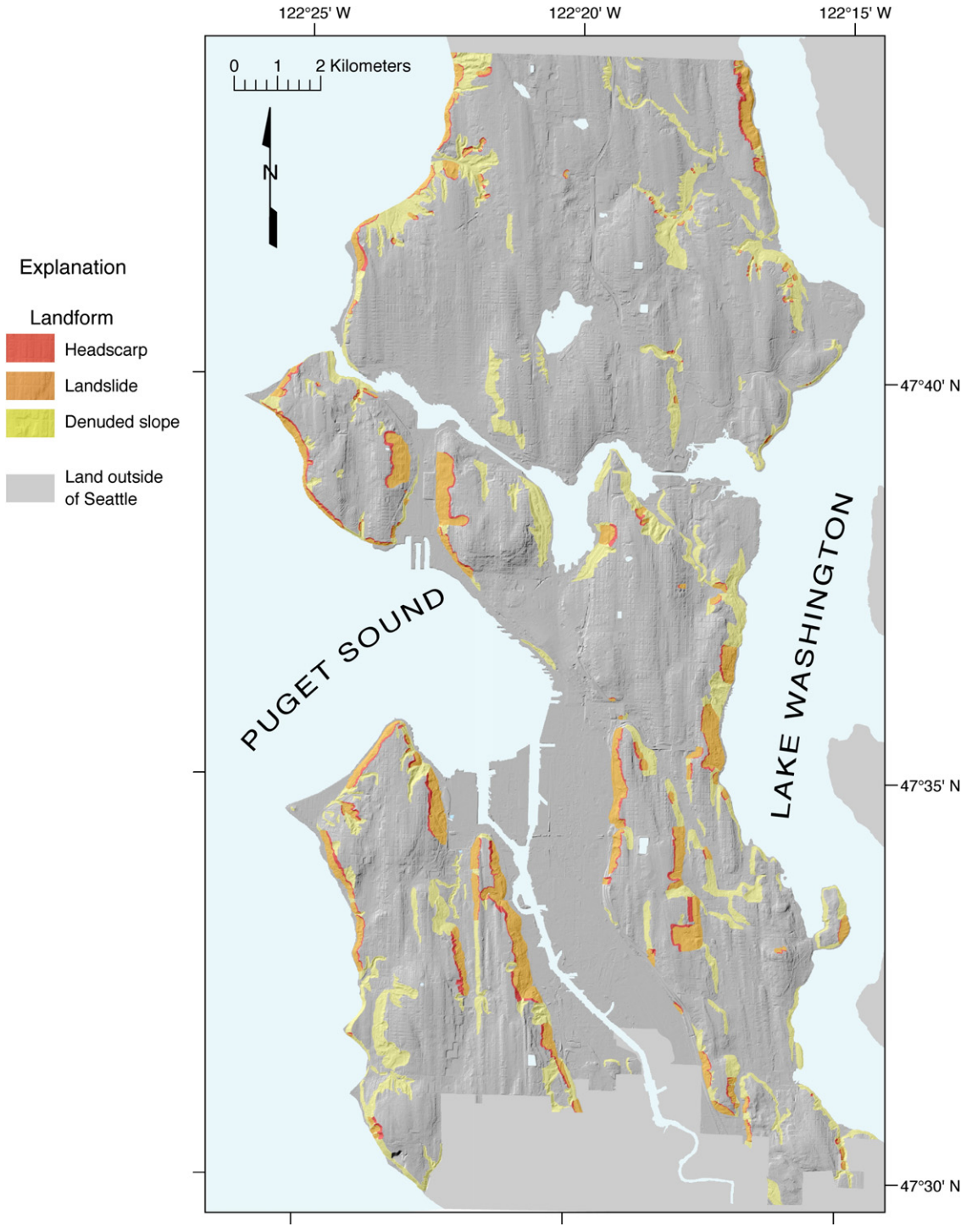

Fig. 9. Landslide-related landforms mapped using LIDAR imagery (Schulz, 2005) draped on a shaded relief map generated from the LIDAR-derived, bare-earth DEM.

These maps and profiles were visually evaluated for topographic characteristics indicative of landslides, such as scarps, hummocky topography, convex and concave slope areas, midslope terraces, and offset drainages. Maps were evaluated at scales ranging from 1:30,000 to 1:2000; mapping was generally performed at 1:5000. Mapped

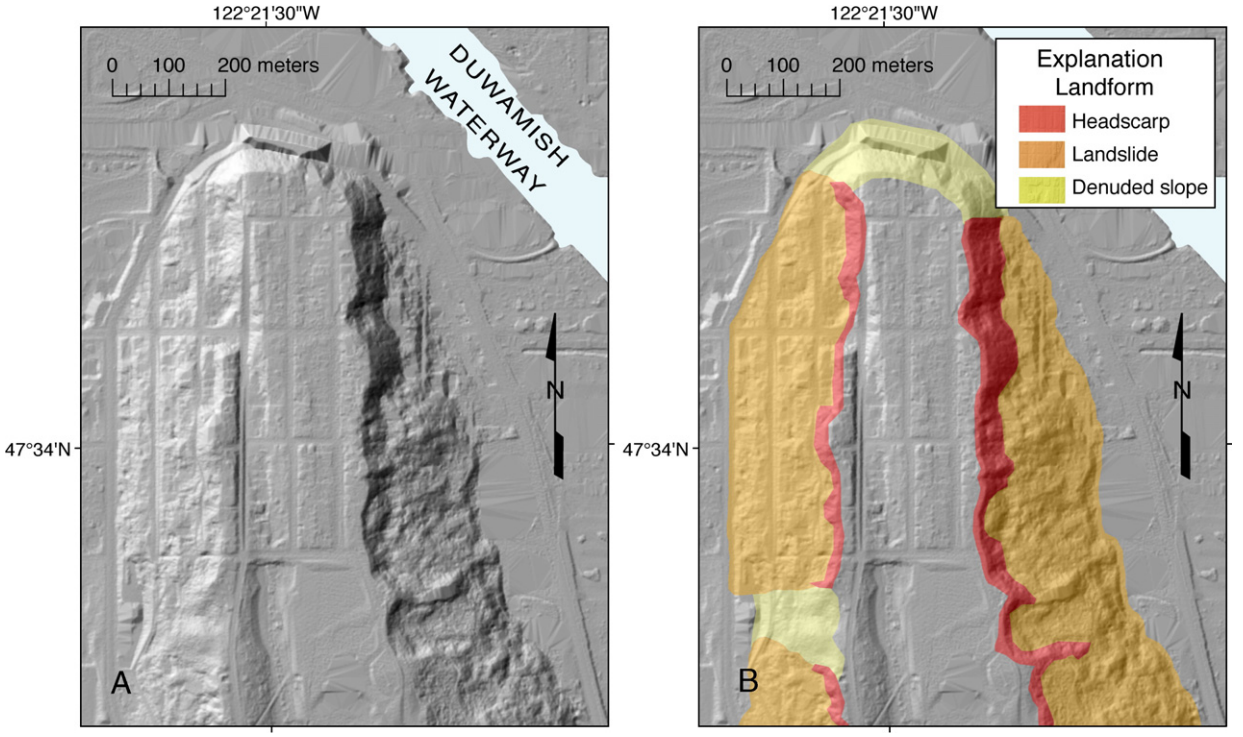

Fig. 10. (A) Shaded relief map of part of Seattle generated from the LIDAR-derived, bare-earth DEM. (B) Landslide-related landforms mapped using LIDAR imagery (Schulz, 2005) draped on the shaded relief map shown on Fig. 10A.

landforms were evaluated in the field during August 2003 and the maps were revised based on field observations, although very little revision was necessary.

3.4. Spatial relations between LIDAR-mapped landforms, stratigraphy, and historical landslides

The spatial densities (in landslides/km^2) of historical landslides by landform were determined using the GIS. Prior to the analysis, mapped landslide landforms were expanded 10 m in all directions, and mapped headscarp and denuded slope landforms were likewise expanded, although not into adjacent landform areas (no overlap exists between the mapped landform areas). This expansion was performed to account for errors in the LIDAR data and in locations of both the mapped landforms and historical landslides. Historical landslides that presumably occurred mostly on the landslide landform were identified as such due to this expansion; historical landslides whose headscarp centers are within 10 m of the initially mapped landslide landform boundaries were identified as occurring on the landslide landform.

The numbers of historical landslides that occurred within stratigraphic units were determined by identifying landslides within the mapped unit boundaries (mapped at 1:12,000 scale) using the GIS. The areas of stratigraphic units corresponding to mapped landforms were also determined using the GIS.

4. Results

LIDAR-derived imagery was used to map 173 landslides and associated headscarps (Fig. 7 and Schulz, 2004). Field evaluation and historical records indicate that nearly all (165 of 173) LIDAR-mapped landslides are actually complexes of multiple landslides.

Landslides and headscarps were classified as uncertain if there was uncertainty regarding the origin of the features. Feature certainty appeared to approximately correlate with activity level with uncertain features being relatively inactive and certain features being relatively active. The total number of landslides mapped using LIDAR is about four times that of previously published maps produced using aerial photographs, and the LIDAR-mapped landslides include all landslides depicted on those maps (Waldron et al., 1962; Waldron, 1967; Youngmann, 1979; Yount et al., 1993; Wait, 2001). Fig. 8 shows results of LIDAR mapping and previous efforts for part of Seattle. The smallest landslide

mapped using LIDAR was just over 20 m across; however, a few larger landslides were identified during ground reconnaissance that had not initially been mapped using the LIDAR imagery. These landslides were in heavily wooded areas and the largest of these landslides was about 30 m across. Landslides were consistently identified using the LIDAR imagery if they had landslide-related topographic features that were at least 30 m long and a few meters high.

Fig. 9 shows the landforms mapped using LIDAR. Fig. 10 shows a large-scale view of map results for part of Seattle illustrating topographic features mapped as landslide-related landforms. Similar to the finding that nearly all LIDAR-mapped landslides and associated headscarps were created by many, much smaller individual landslides, mapped denuded slopes also appear to have been formed by many individual landslides as indicated by intersecting landslide scars observed in the field and evaluation of historical records. The landslide, headscarp, and denuded slope landforms cover 4.6%, 1.2%, and 9.5% of Seattle's land area, respectively. Most (93%) historical landslides occurred on the mapped landforms, and nearly all (99.7%) naturally occurring historical landslides occurred on the landforms.

4.1. LIDAR-mapped landforms, historical landslides, and geologic conditions

All of the stratigraphic units shown on Fig. 5 are represented within the mapped landforms and at the locations of historical landslides (Fig. 11). Forty-nine percent of the landslides mapped using LIDAR intersect the basal contact of the advance outwash (Qva). At least 93% of the LIDAR-mapped landforms are located along coastlines and drainages (including former coastlines and drainages altered by human activity). Fig. 12 shows an example of the distribution of historical landslides, mapped landforms, and stratigraphic conditions in an area that includes the greatest density of historical landslides in Seattle (Coe et al., 2004). Fig. 13 shows an additional example of this distribution. Fig. 14 shows the percentages by stratigraphic unit of historical landslides with various characteristics that occurred on the mapped landforms.

4.2. Landslide features within mapped landforms

The landslides that created the mapped landforms are of variable age and type (e.g., Figs. 12 and 13). Descriptions of the historical landslides shown in Figs. 12 and 13 indicate that they only account for a small part of the total area of the mapped landforms; hence, most of the landslide activity responsible for creation of the landforms was probably prehistoric. Figs. 12A and 13A show that historical landslides are concentrated within the mapped landforms, and appear to generally be located on the steepest parts of slopes. Figs. 12B and 13B illustrate the flat-lying nature of Seattle stratigraphy, the distribution of historical landslides within all slope-comprising stratigraphic units, and, by comparison with Figs. 12A and 13A, indicate that all stratigraphic units are represented in the mapped landforms (except for beach deposits).

Table 1 shows the spatial densities (in landslides/km^2) of historical landslides within each landform area and within the remainder of Seattle (the area in which landslide-related landforms were not identified during mapping and which covers 84.7% of Seattle).

Historical landslide densities increase from the denuded slope landform to the landslide landform, and are greatest for the headscarp landform (Table 1).

The densities of human-caused historical landslides are generally much greater than those of natural historical landslides (Tables 2,3). Table 4 provides ratios of the densities of human-caused historical landslides to the densities of natural historical landslides and shows that human activities are at least partly responsible for causing 7.4 times the number of natural historical landslides. The ratios also indicate the potential for human activity to result in specific types of historical landslides on each of the landforms. Comparison of Tables 3 and 4 shows that, in general, the lower the density of naturally occurring historical landslides on a landform (Table 3), the greater the relative abundance of human-caused historical landslides (as indicated by higher ratios on Table 4). For

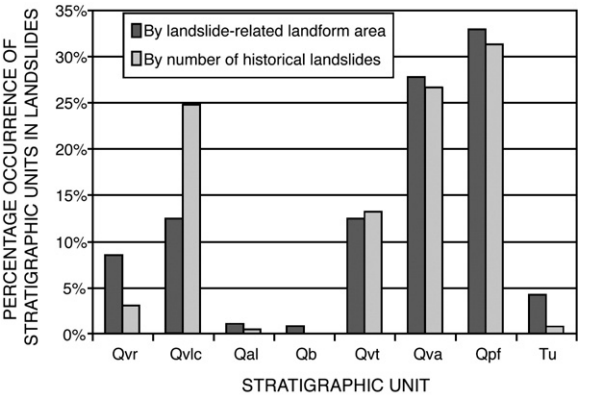

Fig. 11. Landslide occurrence by stratigraphic unit in terms of the percentage of each unit within the landslide-related landforms and in terms of the percentage of the number of historical landslides within each unit.

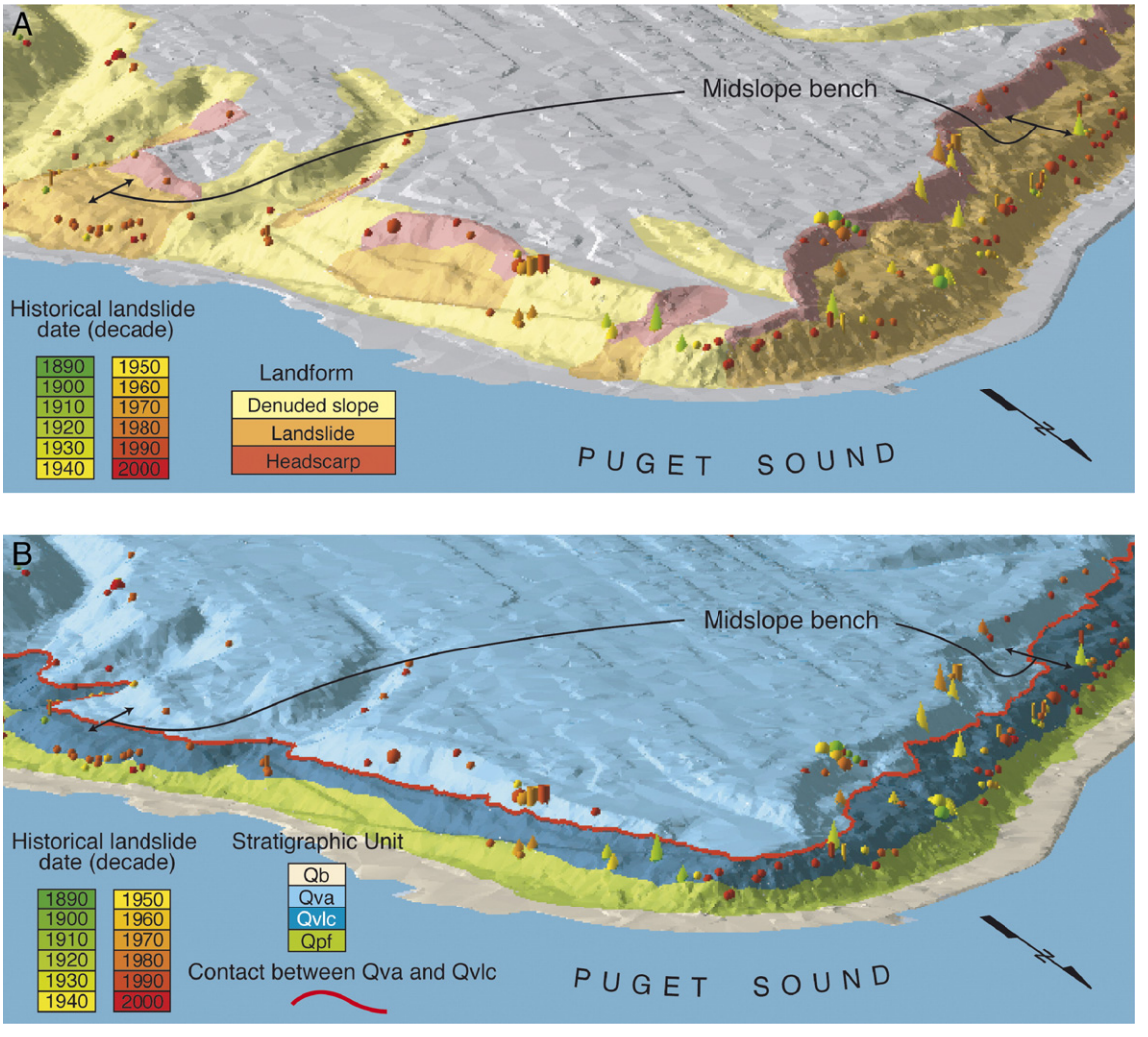

Fig. 12. Oblique aerial view created from the LIDAR-derived, bare-earth DEM. View is toward the south of the Duwamish Head area of Seattle (Fig. 3) and is approximately 1300 m across at the top of the figure. Landslide-related landforms (A), stratigraphic units (B) (simplified version of Troost et al., 2005), and locations of historical landslides (modified from Shannon and Wilson, Inc., 2003) are shown. These locations are represented by colored symbols of variable size; colors indicate the decade during which each landslide occurred. Deep landslides (greater than about 3 m thick) are represented by cones, shallow landslides (less than about 3 m thick) by spheres, and flows by cylinders. Large symbols indicate large landslides (greater than about 930 m^2 in area) while small symbols indicate small landslides (less than about 930 m^2 in area). The midslope bench that occurs along many Seattle slopes is apparent along the bluff in the right third of the figure.

example, the density of all natural historical landslides is least outside of the mapped landform areas (remainder of Seattle) at 0.02 landslides/km^2 and is greatest within the headscarp landform area at 17.58 landslides/km^2 (Table 3), while the ratio of human-caused to natural historical landslides is greatest outside of the mapped landform areas (remainder of Seattle) at 19.0 and is least within the headscarp landform area at 5.6 (Table 4). The greater density of human activities in areas that are less naturally susceptible to landslides (i.e., the relatively flat uplands) may explain this trend in historical landslide density.

The densities of historical landslides within the mapped landforms (Table 1) are essentially equivalent to the relative susceptibilities of the landforms to historical landsliding. The densities should approximate the relative susceptibilities of the landforms to future landsliding, since future landslide activity in Seattle will likely be similar to that of the past (e.g., Thorsen, 1989; Baum et al., 1998; Laprade et al., 2000). The susceptibilities are relative in that they are only meaningful when compared between landforms or landslides with different characteristics in Seattle. For example, Table 1 shows densities

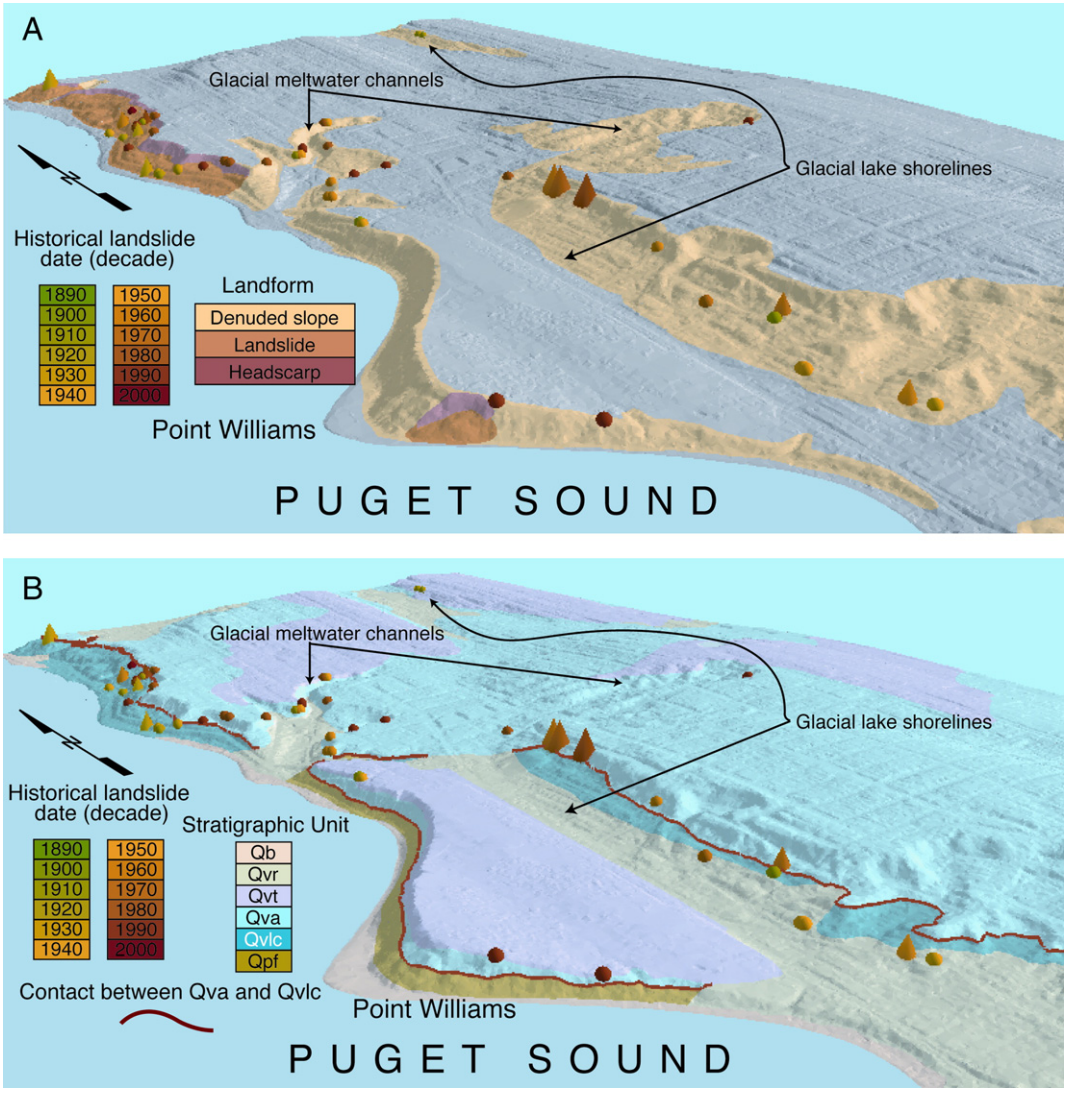

Fig. 13. Oblique aerial view created from the LIDAR-derived, bare-earth DEM. View is toward the northeast and is of the Point Williams area of Seattle (Fig. 3). The land area shown is between 1700–2000 m wide from east to west. Landslide-related landforms (A), stratigraphic units (B) (simplified from Troost et al., 2005), and locations of historical landslides (modified from Shannon and Wilson, Inc., 2003) are shown. These locations are represented by colored symbols of variable size; colors indicate the decade during which each landslide occurred. Deep landslides (greater than about 3 m thick) are represented by cones and shallow landslides (less than about 3 m thick) are represented by spheres. Large symbols indicate large landslides (greater than about 930 m^2 in area) while small symbols indicate small landslides (less than about 930 m^2 in area). Former glacial meltwater channels and glacial lake shorelines are indicated. Point Williams is a park, hence landslides therein are probably rarely reported.

(relative susceptibilities) of 122.23 and 0.47 for the headscarp landform and the remainder of Seattle, respectively. These values suggest that the likelihood of future landslide occurrence on mapped headscarp landforms is 244 times greater than within the remainder of Seattle area. As another example, shallow and deep landslides have densities (relative susceptibilities) of 27.38 and 10.99, respectively, on the landslide landform. Therefore, the likelihood of shallow landsliding is 2.5 times that of deep landsliding on the landslide landform. For comparison, on the headscarp landform, shallow and deep landslides have susceptibilities of 83.08 and 14.78, respectively; therefore, the likelihood of shallow landsliding is 5.6 times that of deep landsliding on the headscarp landform. Hence, the landslide landform is about two times (5.6/2.5) more susceptible than the headscarp landform to deep landsliding relative to shallow landsliding. Comparisons that cannot meaningfully be made

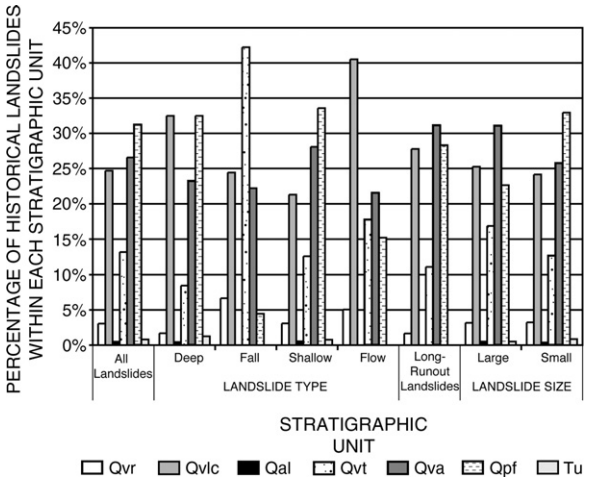

Fig. 14. Percentage of historical landslides that occurred within each stratigraphic unit. Deep landslides are greater than about 3 m thick, shallow landslides are less than about 3 m thick, long-runout landslides have greater than 15 m of rapid displacement, large landslides have area greater than about 930 m^2, and small landslides have area less than about 930 m^2.

include comparing susceptibility values between different landslide feature classes (i.e., type, long-runout, and size).

5. Discussion

5.1. LIDAR-based map utility

Previous landslide mapping efforts in Seattle included geologic mapping for part of Seattle (Waldron, 1967), geologic mapping for all of Seattle (Waldron et al., 1962; Yount et al., 1993), geologic mapping along the Puget Sound coastline of Seattle (Youngmann, 1979), and solely landslide mapping for all of Seattle (Wait, 2001). These efforts included identification of some recent landslides that were not identified using LIDAR, although these recent landslides fall within landslide complexes mapped using LIDAR (Fig. 8). Wait's map (2001) is most applicable for comparison to results of the present study and used 1:2,000–1:2,500-scale black-and-white, color, and color-infrared aerial photographs taken during March 1974, June 1986 and 1991, and September 1995 and 1997. Evaluation of Wait's map (2001), which identified the most landslides of the previous efforts, indicates that aerial photographs were instrumental for identifying recent individual landslides; therefore, aerial photographs appear to be more effective than LIDAR in the Seattle area for discerning boundaries of recently active landslides within landslide complexes. The resolution of the LIDAR data appears to be inadequate to resolve many landslide boundaries within landslide complexes. However, LIDAR was much more effective for identifying presumably older landslides and the boundaries of complexes in which recently active landslides occurred (Fig. 8). For example, of the 128 historical landslides shown in Fig. 8, 124 are located within LIDAR-mapped landslide complexes (including headscarps), while only 19 fall within the boundaries of landslides mapped by Wait (2001). Note that the northern end of the LIDAR-mapped landslide complex in Fig. 8 is absent historical landslides because it is a city park. Landslides in parks typically go unreported because they rarely damage built structures, which partly illustrate the reporting bias of the historical landslide database.

Common to many landslide inventories, the Seattle landslide inventories constructed using LIDAR, aerial photography, and other means (Waldron et al., 1962; Waldron, 1967; Youngmann, 1979; Yount et al., 1993; Wait, 2001; Schulz, 2004) omit many areas prone to landsliding because they omit excavated landslide scars. Denuded slopes appear to primarily consist of coalescing landslide scars and disrupted, thin landslide deposits. Over 37% of historical landslides in Seattle occur on LIDAR-mapped denuded slopes, thus denuded slopes should be considered in regional evaluations of landslide susceptibility.

5.2. Occurrence of landslides in Seattle

The occurrence of Seattle landslides does not appear to be spatially related to stratigraphic conditions (Figs. 11–13). Most Seattle landslides occur in pre-Fraser deposits (Qpf), advance outwash (Qva), Lawton Clay (Qvlc), and till (Qvt), and do not preferentially occur to a significant extent in any of these units (Fig. 11). These stratigraphic units typically comprise Seattle's high, steep hillsides that extend from near sea level to the upland surface (Fig. 5). It appears that the relative number of landslides within each stratigraphic unit is directly proportional to the relative amount of land area underlain by each unit along Seattle's high, steep hillsides (Figs. 5 and 11). This contradicts the conclusion that the basal contact of the advance outwash (Qva) defines a zone where most landslides occur in Seattle (Tubbs, 1974, 1975). Although 29% of historical landslides occur within the 61-m-wide strip centered along this basal contact (as mapped by Troost et al., 2005), they only do so where the contact coincides with a mapped landform; 64% of historical landslides occur within mapped landforms that are absent the contact strip. Historical landslides do not occur within the part of the contact strip that occurs outside of the mapped landforms (24% of the contact strip area). The presence of landslides near the contact appears to be coincidental; advance

Table 1
Densities of historical Seattle landslides (landslides/km^2)

Location	All Landslides	Shallow [a] landslides	Deep [b] landslides	Flows	Falls	Long-runout [c] landslides	Large [d] landslides	Small [e] landslides
Headscarp landform	122.23	83.08	14.78	10.39	9.19	22.77	23.17	93.47
Landslide landform	42.77	27.38	10.99	3.40	0.60	5.80	7.00	34.08
Denuded slope landform	23.74	17.75	3.50	0.88	0.78	2.87	2.68	19.80
Remainder of Seattle	0.47	0.35	0.10	0.01	0.00	0.03	0.04	0.41
All of Seattle	6.07	4.23	1.10	0.37	0.21	0.83	0.88	4.90

Note: Some density values in this table are greater than the sums of densities of human-caused and natural landslides (Tables 2 and 3) because this table includes landslides for which the cause is unknown.
[a] Shallow landslides are less than about 3-m thick.
[b] Deep landslides are greater than about 3-m thick.
[c] Long-runout landslides have greater than 15 m of rapid displacement.
[d] Large landslides are greater than 930 m^2 in area.
[e] Small landslides are less than 930 m^2 in area.

outwash (Qva) is present nearly everywhere beneath Seattle (Fig. 5) and its stratigraphic position dictates that its basal contact occurs along most high, steep slopes (e.g., Figs. 12,13). Tubbs' (1974, 1975) conclusion that landslides preferentially occur near the base of an aquifer (i.e., the base of the advance outwash) is based on sound reasoning. Elevated groundwater pore pressures do trigger Seattle landslides; however, they cannot cause landslides in the absence of a slope (excluding liquefaction-type failures).

Natural historical landslides essentially all (99.7%) occurred within the mapped landform boundaries. One condition was identified at the locations of nearly all of the mapped landforms; surface water eroded slope toes at some time since retreat of glacial ice. This erosion is of highly variable age and occurred along glacial lakeshores, glacial meltwater streams, recent streams, and the coasts of Lake Washington and Puget Sound. Figs. 12 and 13 illustrate the apparent relationship between surface-water erosion of slope toes and the locations of landslides. Landslides have been concentrated along former and present surface-water bodies and have not occurred elsewhere.

Landsliding due to surface-water erosion of slope toes has well known characteristics (e.g., Quigley et al., 1977; Edil and Vallejo, 1980; Buckler and Winters, 1983; Vallejo and Degroot, 1988; Hampton et al., 2004). Erosion of slope toes removes supporting materials and thereby reduces the shear strength available to resist landsliding (e.g., Terzaghi, 1950; Hutchinson, 1968; Quigley et al., 1977; Vallejo and Degroot, 1988; Hampton et al., 2004; Shipman, 2004). Landslides that form due to slope-toe erosion remove support for upslope areas, which similarly fail. Landslides progressively occur upslope until the slope crest fails. Concurrent with the progressive failures, landslide debris that reaches the slope toe is eroded by surface water, which undermines upslope landslide debris and underlying native deposits, making them fail. This cycle continues while slope-toe erosion is active, and the result is essentially parallel retreat of the failing slopes. If erosion ceases, landslide deposits accumulate along the lower parts of slopes and

Table 2
Densities of human-caused historical Seattle landslides (landslides/km^2)

Location	All landslides	Shallow [a] landslides	Deep [b] landslides	Flows	Falls	Long-runout [c] landslides	Large [d] landslides	Small [e] landslides
Headscarp landform	98.26	69.90	11.58	10.39	6.39	20.37	20.77	77.49
Landslide landform	35.18	21.89	9.69	3.30	0.30	5.40	6.40	28.58
Denuded slope landform	20.18	15.47	3.31	0.68	0.58	2.58	2.43	17.66
Remainder of Seattle	0.42	0.31	0.10	0.01	0.00	0.03	0.04	0.37
All of Seattle	5.05	3.56	0.99	0.34	0.14	0.76	0.80	4.22

[a] Shallow landslides are less than about 3-m thick.
[b] Deep landslides are greater than about 3-m thick.
[c] Long-runout landslides have greater than 15 m of rapid displacement.
[d] Large landslides are greater than 930 m^2 in area.
[e] Small landslides are less than 930 m^2 in area.

Table 3
Densities of natural historical Seattle landslides (landslides/km^2)

Location	All landslides	Shallow [a] landslides	Deep [b] landslides	Flows	Falls	Long-runout [c] landslides	Large [d] landslides	Small [e] landslides
Headscarp landform	17.58	8.39	2.00	0.00	2.80	2.00	2.40	9.59
Landslide landform	5.30	3.80	0.70	0.10	0.30	0.30	0.30	4.00
Denuded slope Landform	2.24	1.22	0.19	0.10	0.15	0.10	0.24	1.12
Remainder of Seattle	0.02	0.01	0.00	0.00	0.00	0.00	0.00	0.01
All of Seattle	0.68	0.40	0.07	0.01	0.06	0.05	0.06	0.41

[a] Shallow landslides are less than about 3-m thick.
[b] Deep landslides are greater than about 3-m thick.
[c] Long-runout landslides have greater than 15 m of rapid displacement.
[d] Large landslides are greater than 930 m^2 in area.
[e] Small landslides are less than 930 m^2 in area.

reduce the slope inclinations, which increases slope stability. As slope inclinations decrease along the lower parts of slopes, landslides progressively concentrate near the slope crests until crest inclinations also decrease to a point of stability due to evacuation of landslide debris. Natural landsliding essentially ceases at that time.

In a setting as is present in Seattle where slope-toe erosion results in landslides, stratigraphic conditions can affect landslide characteristics (Fig. 14) and slope morphology. Perhaps the strongest evidence of these effects in Seattle are the midslope topographic benches often located near the top of the Lawton Clay (Qvlc) (e.g., Figs. 12,13), which can be explained as follows. Surface-water erosion of slope toes has generally occurred within pre-Fraser deposits (Qpf) and Lawton Clay (Qvlc) because of their stratigraphic position. Landslides in pre-Fraser deposits (Qpf) and Lawton Clay (Qvlc) that result from this erosion are generally small (Fig. 14) and undermine upslope areas. This undermining causes landslides in advance outwash (Qva) and overlying till (Qvt), which are generally large (Fig. 14). Because landslides are generally large in the advance outwash (Qva) and till (Qvt) and those in underlying units are generally small, landslides in the advance outwash (Qva) and till (Qvt) may result in more rapid, though episodic retreat of the upper part of slopes, thus forming the topographic benches. Deposits of landslides from the advance outwash (Qva) and till (Qvt) accumulate on the benches and downslope, and were generally mapped as landslide landforms during the present study. The escarpments formed by these landslides were generally mapped as headscarp landforms. Landslide deposits that accumulate on benches may partly buttress escarpments located upslope, resulting in a period of increased slope stability along headscarps. Landsliding continues downslope of the bench during this period as slope-toe erosion by surface water continues, resulting in additional retreat of pre-Fraser deposits (Qpf) and Lawton Clay (Qvlc). Fig. 12 illustrates this greater concentration of landslides downslope from benches than on headscarps, even though slope-toe erosion has been arrested in this area for about one hundred years by human activity. Retreat of the slope below the bench progressively undermines deposits on the bench and upslope and may result in complete removal of the bench, possibly forming a denuded slope. Future landslide activity results in

Table 4
Ratios of human-caused landslide densities to natural landslide densities in Seattle

Location	All landslides	Shallow [a] landslides	Deep [b] landslides	Flows	Falls	Long-runout [c] landslides	Large [d] landslides	Small [e] landslides
Headscarp landform	5.6	8.3	5.8	All HC	2.3	10.2	8.7	8.1
Landslide landform	6.6	5.8	13.9	33.0	1.0	18.0	21.3	7.2
Denuded slope landform	9.0	12.7	17.0	7.0	4.0	26.5	10.0	15.8
Remainder of Seattle	19.0	28.0	All HC	None	None	None	None	33.5
All of Seattle	7.4	8.9	13.3	24.7	2.4	16.4	12.4	10.2

Note: "All HC" indicates that all landslides were human caused; "None" indicates no landslides were reported.
[a] Shallow landslides are less than about 3-m thick.
[b] Deep landslides are greater than about 3-m thick.
[c] Long-runout landslides have greater than 15 m of rapid displacement.
[d] Large landslides are greater than 930 m^2 in area.
[e] Small landslides are less than 930 m^2 in area.

additional slope retreat and possible repeated cycles of bench creation and destruction.

Landslide activity will not cease concurrent with cessation of slope-toe erosion because slopes whose toes were eroded will require time to naturally stabilize through landsliding, as described above. Landslides have occurred in Seattle for more than one hundred years after human activities arrested slope-toe erosion (Fig. 12), thus more time than this is required to achieve stability. This is not surprising because most landslide-susceptible slopes in Seattle are of much greater extent than typical Seattle landslides (e.g., Fig. 6) so individual landslides do little to stabilize slopes. Seattle landslide complexes and denuded slopes whose formation initiated during glacial melt-off (e.g., Fig. 13) provide analogs to areas where slope-toe erosion has recently ceased. Overall slope inclinations appear to be more gentle and historical landslide activity appears to be reduced in areas that have been free of slope-toe erosion since soon after deglaciation compared to areas of recent slope-toe erosion (Fig. 13; note that Point Williams is a park, hence landslides therein may generally be unreported, similar to the park in the northern part of Fig. 8). However, historical landslides have occurred in the areas free of slope-toe erosion since deglaciation. Therefore, more than about 16,400 years is required to naturally achieve slope stability in Seattle, given past climatic conditions. It does not appear that human-constructed, slope-toe erosion protection has made significant impact on landslide activity to date, as suggested by the temporal and spatial distributions of landslides shown on Fig. 12. This figure shows the Seattle bluff area that has been protected from slope-toe erosion by human activity for the greatest length of time, yet landslides still occur low on the bluff.

6. Conclusions

Imagery derived from LIDAR data was used to identify and map about four times more landslides in Seattle than had been mapped previously using aerial photographs. Landslides mapped using LIDAR mainly consist of many smaller landslides that occurred during both prehistoric and historic times, and as such are landslide complexes. LIDAR imagery was also effective for mapping denuded slopes, which are mainly produced by landslides and are susceptible to future landsliding. Nearly all mapped landslide complexes, headscarps, and denuded slopes are located along slopes that have been subjected to toe erosion by wave action or stream flow.

Locations of historical landslides are heavily concentrated on mapped landslide, headscarp, and denuded slope landforms; 99.7% of natural historical landslides occur on these landforms. Historical landslide spatial densities are related to landform type. These densities are greatest along the headscarp landform and decrease to the landslide landform and then to the denuded slope landform. The landforms were primarily created by prehistoric landslide activity, so the concentration of historical landslide activity on mainly prehistoric landforms indicates that landslide locations have been consistent in recent times. It follows that future activity will be similar, so the spatial densities of historical landslides on the landforms were used to generate a landslide susceptibility map. This map indicates the relative susceptibility to landslides with different characteristics occurring on each of the landforms and in the area outside of them. Areas outside of the mapped landforms are virtually unsusceptible to landslides; landslide susceptibility on the landforms is about 47 to 244 times greater than that outside the landforms.

The concentration of historical landslides on LIDAR-mapped landforms, the distribution of these landforms along current and former surface-water bodies, and observed bluff retreat in Seattle indicate that slope-toe erosion was a necessary condition for forming Seattle landslides, and its effects continue to result in landslides. There appears to be little stratigraphic control on the occurrence of landslides in Seattle; the number of historical landslides that occurred on three of the four primary stratigraphic units present along most Seattle hillsides differs by just 6% and appears to be directly proportional to the distribution of the units on susceptible hillsides. This apparent lack of stratigraphic control on landslide occurrence conflicts with the generally accepted theory that landslides in Seattle typically occur due to conditions present near the basal contact of the advance outwash. Evaluation of the distribution of the contact, mapped landforms, and historical landslides indicates that historical landslides only occur near the contact where its location coincides with a mapped landform. The presence of the contact near historical landslides appears to be coincidental. Stratigraphic control on landslide characteristics and slope morphology is evident, however.

Future landslide activity in Seattle is expected to be similar in style and location to recent activity. Erosion of most slope toes in Seattle has been arrested by human activity. This will result in a reduction in landslide activity starting from the lower parts of slopes and progressing upslope as hillside inclinations are reduced by landsliding. However, evaluation of the distributions of historical landslides in areas where glacial meltwater eroded slope toes indicates that 16,400 years without

slope-toe erosion has been insufficient for hillsides to naturally self-stabilize. In addition, man's removal of landslide debris on the lower parts of slopes serves the same purpose as erosion; stabilization of hillsides by accumulation of landslide deposits near their bases is not allowed to occur. However, humans have accelerated the process of slope evolution by partly causing about 80% of Seattle's landslides (Shannon and Wilson, Inc., 2003), so the ultimate stabilization of Seattle's hillsides through landsliding may require less time than if landsliding was purely natural. Clearly, landslides in Seattle will continue to pose hazards for the foreseeable future. The areas in which landslide susceptibility is greatest and the kinds of landslides that will likely occur in specific areas have been identified by mapping landslide-related landforms using LIDAR.

References

Armstrong, J.E., Crandell, D.R., Easterbrook, D.J., Noble, J.B., 1965. Late Pleistocene stratigraphy and chronology in southwestern British Columbia and northwestern Washington. Geological Society of America Bulletin 76, 321–330.

Bates, R.L., Jackson, J.A., 1987. Glossary of Geology. American Geological Institute, Alexandria, Va. 788 pp.

Baum, R.L., Chleborad, A.F., Schuster, R.L., 1998. Landslides triggered by the winter 1996–97 storms in the Puget Lowland, Washington. U.S. Geological Survey Open-File Report 98–239. 16 pp.

Booth, D.B., 1987. Timing and processes of deglaciation along the southern margin of the Cordilleran ice sheet. In: Ruddiman, W.F., Wright Jr., H.E. (Eds.), North America and Adjacent Oceans During the Last Deglaciation; The Geology of North America, K-3. Geological Society of America, Boulder, Colorado, pp. 71–90.

Booth, D.B., Troost, K.G., Shimel, S.A., 2000. The Quaternary geologic framework for the city of Seattle and the Seattle-Tacoma urban corridor. U.S. Geological Survey Final Technical Report. 24 pp.

Booth, D.B., Troost, K.G., Shimel, S.A., 2005. Geologic map of northwestern Seattle (part of the Seattle north 7.5′×15′ quadrangle), King County, Washington. U.S. Geological Survey Scientific Investigations Map 2903.

Buckler, W.R., Winters, H.A., 1983. Lake Michigan bluff recession. Annals of the Association of American Geographers 73 (1), 89–110.

Chleborad, A.F., 2000. Preliminary methods for anticipating the occurrence of precipitation-induced landslides in Seattle, Washington. U.S. Geological Survey Open-File Report 00 -0469. 29 pp.

Coe, J.A., Michael, J.A., Crovelli, R.A., Savage, W.Z., 2000. Preliminary map showing landslide densities, mean recurrence intervals, and exceedance probabilities as determined from historic records, Seattle, Washington. U.S. Geological Survey Open-File Report 00-303. 25 pp., 1 sheet.

Coe, J.A., Michael, J.A., Crovelli, R.A., Savage, W.Z., Laprade, W.T., Nashem, W.D., 2004. Probabilistic assessment of precipitation-triggered landslides using historical records of landslide occurrence, Seattle, Washington. Environmental and Engineering Geoscience 10 (2), 103–122.

Cruden, D.M., Varnes, D.J., 1996. Landslide types and processes. In: Turner, A.K., Schuster, R.L. (Eds.), Landslides, Investigation and Mitigation: Transportation Research Board Special Report, vol. 247. National Research Council, Washington, D.C., pp. 36–75.

Edil, T.B., Vallejo, L.E., 1980. Mechanics of coastal landslides and the influence of slope parameters. Engineering Geology 16, 83–96.

Galster, R.W., Laprade, W.T., 1991. Geology of Seattle, Washington, United States of America. Bulletin of the Association of Engineering Geologists 28 (3), 235–302.

Gerstel, W.J., Brunengo, M.J., Lingley Jr., W.S., Logan, R.L., Shipman, H., Walsh, T.J., 1997. Puget Sound bluffs: the where, why, and when of landslides following the holiday 1996/97 storms. Washington Geology 25 (1), 17–31.

Hampton, M.A., Griggs, G.B., Edil, T.B., Guy, D.E., Kelley, J.T., Komar, P.D., Mickelson, D.M., Shipman, H.M., 2004. Processes that govern the formation and evolution of coastal cliffs. In: Hampton, M.A., Griggs, G.B. (Eds.), Formation, Evolution, and Stability of Coastal Cliffs — Status and Trends. U.S. Geological Survey Professional Paper, vol. 1693, pp. 7–38.

Harp, E.L., Chleborad, A.F., Schuster, R.L., Cannon, S.H., Reid, M.E., Wilson, R.C., 1996. Landslides and landslide hazards in Washington State due to February 5–9, 1996 storm. U.S. Geological Survey Administrative Report. 29 pp.

Haugerud, R.A., Harding, D.J., 2001. Some algorithms for virtual deforestation (VDF) of LIDAR topographic survey data. International Archives of Photogrammetry and Remote Sensing XXXIV-3/W4, 211–217.

Haugerud, R.A., Harding, D.J., Johnson, S.Y., Harless, J.L., Weaver, C.S., Sherrod, B.L., 2003. High-resolution LIDAR topography of the Puget Lowland, Washington. GSA Today 13 (6), 4–10.

Highland, L.M., 2003. An account of preliminary landslide damage and losses resulting from the February 28, 2001, Nisqually, Washington, Earthquake. U.S. Geological Survey Open-file Report 03-211. 48 pp.

Hutchinson, J.N., 1968. Field meeting on the coastal landslides of Kent. Proceedings, Geotechnical Conference of Oslo, vol. 1, pp. 113–118.

Johnson, S.Y., Nelson, A.R., Personius, S.F., Wells, R.E., Kelsey, H.M., Sherrod, B.L., Okumura, K., Koehler, R., Witter, R., Bradley, L., Harding, D.J., 2003. Maps and data from a trench investigation of the Utsalady Point fault, Whidbey Island, Washington. U.S. Geological Survey Miscellaneous Field Studies Map MF-2420. 1 sheet.

Laprade, W.T., Kirkland, T.E., Nashem, W.D., Robertson, C.A., 2000. Seattle landslide study. Shannon and Wilson, Inc. Internal Report W-7992 -01. 164 pp.

Ludwin, R.S., Thrush, C.P., James, K., Buerge, D., Jonientz-Trisler, C., Rasmussen, J., Troost, K., de los Angeles, A., 2005. Serpent spirit-power stories along the Seattle fault. Seismological Research Letters 76 (4), 426–431.

Miller, D.J., 1991. Damage in King County from the storm of January 9, 1990. Washington Geology 19 (1), 28–37.

Montgomery, D.R., Greenberg, H.M., Laprade, W.T., Nashem, W.D., 2001. Sliding in Seattle: test of a model of shallow landsliding potential in an urban environment. In: Wigmosta, M.S., Burges, S.J. (Eds.), Land Use and Watersheds, Human Influence on Hydrology and Geomorphology in Urban and Forest Areas. American Geophysical Union, Washington, D.C., pp. 59–72.

Mullineaux, D.R., Waldron, H.H., Rubin, M., 1965. Stratigraphy and chronology of late interglacial and Early Vashon glacial time in the Seattle area, Washington. U.S. Geological Survey Bulletin 1194-O. 11 pp.

Newcomb, R.C., 1952. Ground-water resources of Snohomish County, Washington. U.S. Geological Survey Water-Supply Paper 1135. 133 pp.

Quigley, R.M., Gelinas, P.J., Bou, W.T., Packer, R.W., 1977. Cyclic erosion-instability relationships: Lake Erie north shore bluffs. Canadian Geotechnical Journal 14, 310–323.

Savage, W.Z., Morrissey, M.M., Baum, R.L., 2000. Geotechnical properties for landslide-prone Seattle-area glacial deposits. U.S. Geological Survey Open-File Report 00-228. 5 pp.

Schulz, W.H., 2004. Landslides mapped using LIDAR imagery, Seattle, Washington. U.S. Geological Survey Open-File Report 2004-1396. 11 pp., 1 plate.

Schulz, W.H., 2005. Landslide susceptibility estimated from LIDAR mapping and historical records for Seattle, Washington. U.S. Geological Survey Open-File Report 2005-1405. 16 pp., 1 plate.

Shannon and Wilson, Inc., 2003. Seattle landslide study update, addendum to the Seattle landslide study, stability improvement areas. Unpublished consultant report 21-1-08913 - 016, for Seattle Public Utilities, Seattle, Wash., 12 pp.

Sherrod, B.L., Bucknam, R.C., Leopold, E.B., 2000. Holocene relative sea level changes along the Seattle Fault at Restoration Point, Washington. Quaternary Research 54, 384–393.

Sherrod, B.L., Brocher, T.M., Weaver, C.S., Bucknam, R.C., Blakely, R.J., Kelsey, H.M., Nelson, A.R., Haugerud, R., 2004. Holocene fault scarps near Tacoma, Washington, USA. Geology 32 (1), 9–12.

Shipman, H., 2004. Coastal bluffs and sea cliffs on Puget Sound, Washington. In: Hampton, M.A., Griggs, G.B. (Eds.), Formation, Evolution, and Stability of Coastal Cliffs — Status and Trends. U.S. Geological Survey Professional Paper, vol. 1693, pp. 81–94.

Terzaghi, K., 1950. Mechanism of landslides. In: Paige, Sidney (Chairman), Application of Geology to Engineering Practice, Berkey volume. New York, The Geological Society of America, 83–123.

Thorsen, G.W., 1989. Landslide provinces in Washington. In: Galster, R.W. (Chairman), Engineering Geology in Washington. Washington Division of Geology and Earth Resources Bulletin 78, 71–86.

Troost, K.G., Booth, D.B., Wisher, A.P., Shimel, S.A., 2005. The geologic map of Seattle — a progress report. U.S. Geological Survey Open-File Report 2005-1252. 1 plate.

Tubbs, D.W., 1974. Landslides in Seattle. Washington Division of Geology and Earth Resources Information Circular, vol. 52. 15 pp., 1 plate.

Tubbs, D.W., 1975. Causes, mechanisms and prediction of landsliding in Seattle. Seattle, University of Washington, Ph.D. dissertation, 89 p., 1 plate.

Vaccaro, J.J., Hansen Jr., A.J., Jones, M.A., 1998. Hydrogeologic framework of the Puget Sound aquifer system, Washington and British Columbia. U.S. Geological Survey Professional Paper 1424-D. 77 pp., 1 plate.

Vallejo, L.E., Degroot, R., 1988. Bluff response to wave action. Engineering Geology 26, 1–16.

Wait, T.C., 2001. Charact eristics of deep-seated landslides in Seattle, Washington. Golden, Colorado School of Mines, M.S. thesis, 131 p., 3 plates.

Waldron, H.H., 1967. Geologic map of the Duwamish Head quadrangle, King and Kitsap Counties, Washington. U.S. Geological Survey Geologic Quadrangle GQ-706. 1 plate.

Waldron, H.H., Leisch, B.A., Mull ineaux, D.R., Crandell, D.R., 1962. Preliminary geologic map of Seattle and vicinity, Washington. U.S. Geological Survey Miscellaneous Geologic Investigations Map I-3 54. 1 plate.

Youngmann, C. (Ed.), 1979. King County: Coastal Zone Atlas of Washington. Washington Department of Ecology, Olympia. 9 plates.

Yount, J.C., Minard, J.P., Dembroff, G.R., 1993. Geologic map of surficial deposits in the Seattle 30′ by 60′ quadrangle, Washington. U.S. Geological Survey Open-File Report 93 –233. 3 plates.